LETTERS
https://doi.org/10.1038/s41565-019-0539-2
nature nanotechnology

A biodegradable nanocapsule delivers a Cas9 ribonucleoprotein complex for in vivo genome editing

Guojun Chen[1,2,8], Amr A. Abdeen[2,8], Yuyuan Wang[1,2,8], Pawan K. Shahi[3], Samantha Robertson[4], Ruosen Xie[1,2], Masatoshi Suzuki[4,5], Bikash R. Pattnaik[3,6], Krishanu Saha[2,5*] and Shaoqin Gong[1,2,5,7*]

Delivery technologies for the CRISPR-Cas9 (CRISPR, clustered regularly interspaced short palindromic repeats) gene editing system often require viral vectors, which pose safety concerns for therapeutic genome editing[1]. Alternatively, cationic liposomal components or polymers can be used to encapsulate multiple CRISPR components into large particles (typically >100 nm diameter); however, such systems are limited by variability in the loading of the cargo. Here, we report the design of customizable synthetic nanoparticles for the delivery of Cas9 nuclease and a single-guide RNA (sgRNA) that enables the controlled stoichiometry of CRISPR components and limits the possible safety concerns in vivo. We describe the synthesis of a thin glutathione (GSH)-cleavable covalently crosslinked polymer coating, called a nanocapsule (NC), around a preassembled ribonucleoprotein (RNP) complex between a Cas9 nuclease and an sgRNA. The NC is synthesized by in situ polymerization, has a hydrodynamic diameter of 25 nm and can be customized via facile surface modification. NCs efficiently generate targeted gene edits in vitro without any apparent cytotoxicity. Furthermore, NCs produce robust gene editing in vivo in murine retinal pigment epithelium (RPE) tissue and skeletal muscle after local administration. This customizable NC nanoplatform efficiently delivers CRISPR RNP complexes for in vitro and in vivo somatic gene editing.

Cas9 RNP is an attractive non-viral formulation for CRISPR-mediated gene editing due to its quick DNA cleavage activity, low off-target effects[1,2], low risk of insertional mutagenesis and ease of production[3]. Furthermore, RNPs do not rely on transcriptional or translational cellular machinery for the precise enzymatic gene editing activity, nor carry any long nucleic acids or viral-based approaches that could integrate into the genome. However, existing non-viral strategies for the delivery of Cas9 RNP face a number of challenges[4–7], such as a high cytotoxicity, poor in vivo stability, large particle sizes, lack of specific tissue- and/or cell-targeting abilities, variable loading of the RNP cargo and potential immunogenicity. These challenges limit the application of RNPs for gene editing in vitro, and especially in vivo where chemically-defined stable and off-the-shelf formulations could be critical for translational somatic gene editing applications[1].

We sought to develop a customizable and efficient nanoplatform to deliver Cas9 RNP complexes for both in vitro and in vivo applications. Our design criteria include a high RNP loading content, small nanoparticle sizes, controllable stoichiometry, excellent stability, endosomal escape capability, efficient RNP release once inside the cytosol and amenability to surface modifications. As shown in Fig. 1a, because the RNP exhibits heterogeneous surface charges on the Cas9 protein and sgRNA[5], we posited that a mixture of cationic and anionic monomers (i and ii, respectively) could form a coating around the RNP through electrostatic interactions. An imidazole-containing monomer (iii), GSH-degradable crosslinker (iv), acrylate methoxypoly(ethylene glycol) (mPEG) (v) and acrylate poly(ethylene glycol) (PEG) conjugated with ligands (vi) can also be attracted to the surface of the RNP complex via hydrogen bonding and van der Waals interactions[8,9]. After monomer coating, subsequent in situ free-radical polymerization[8–10] was initiated to form a covalently linked, yet GSH cleavable, NC around the RNP. The integration of the imidazole-containing monomer can facilitate the endosomal escape of the NCs owing to the proton sponge effect of the imidazole groups[11]. NCs were crosslinked with a GSH-cleavable linker, *N*,*N*′-bis(acryloyl)cystamine (BACA), which can be degraded in GSH-rich environments such as the cytosol (2–10 mM (refs [12,13])), and thereby enable the release of RNPs within the cytosol (Fig. 1b). The RNPs can then enter the nucleus, which may be further facilitated by nuclear localization signals (NLSs) fused to the recombinant Cas9 protein[14]. The outer water-soluble PEG shell adds flexibility to conjugate functional moieties, such as targeting ligands, cell penetrating peptides (CPPs), or imaging probes.

To find the optimal monomer stoichiometry for an efficient cellular transfection, the amounts of various monomers were adjusted systematically, as summarized in Fig. 1c. Several critical factors were investigated, which included the anionic/cationic monomer ratio, the amounts of the imidazole-containing monomer and crosslinker and the mass ratio between the NC and RNP. The functionalities of NCs with different formulations were tested on a human embryonic kidney (HEK 293) cell line with an H2B-mCherry transgene

[1]Department of Materials Science and Engineering, University of Wisconsin–Madison, Madison, WI, USA. [2]Wisconsin Institute for Discovery, University of Wisconsin–Madison, Madison, WI, USA. [3]Department of Pediatrics, University of Wisconsin–Madison, Madison, WI, USA. [4]Department of Comparative Biosciences, University of Wisconsin–Madison, Madison, WI, USA. [5]Department of Biomedical Engineering, University of Wisconsin–Madison, Madison, WI, USA. [6]Department of Ophthalmology and Visual Sciences, University of Wisconsin–Madison, Madison, WI, USA. [7]Department of Chemistry, University of Wisconsin–Madison, Madison, WI, USA. [8]These authors contributed equally: Guojun Chen, Amr A. Abdeen, Yuyuan Wang.
*e-mail: ksaha@wisc.edu; shaoqingong@wisc.edu

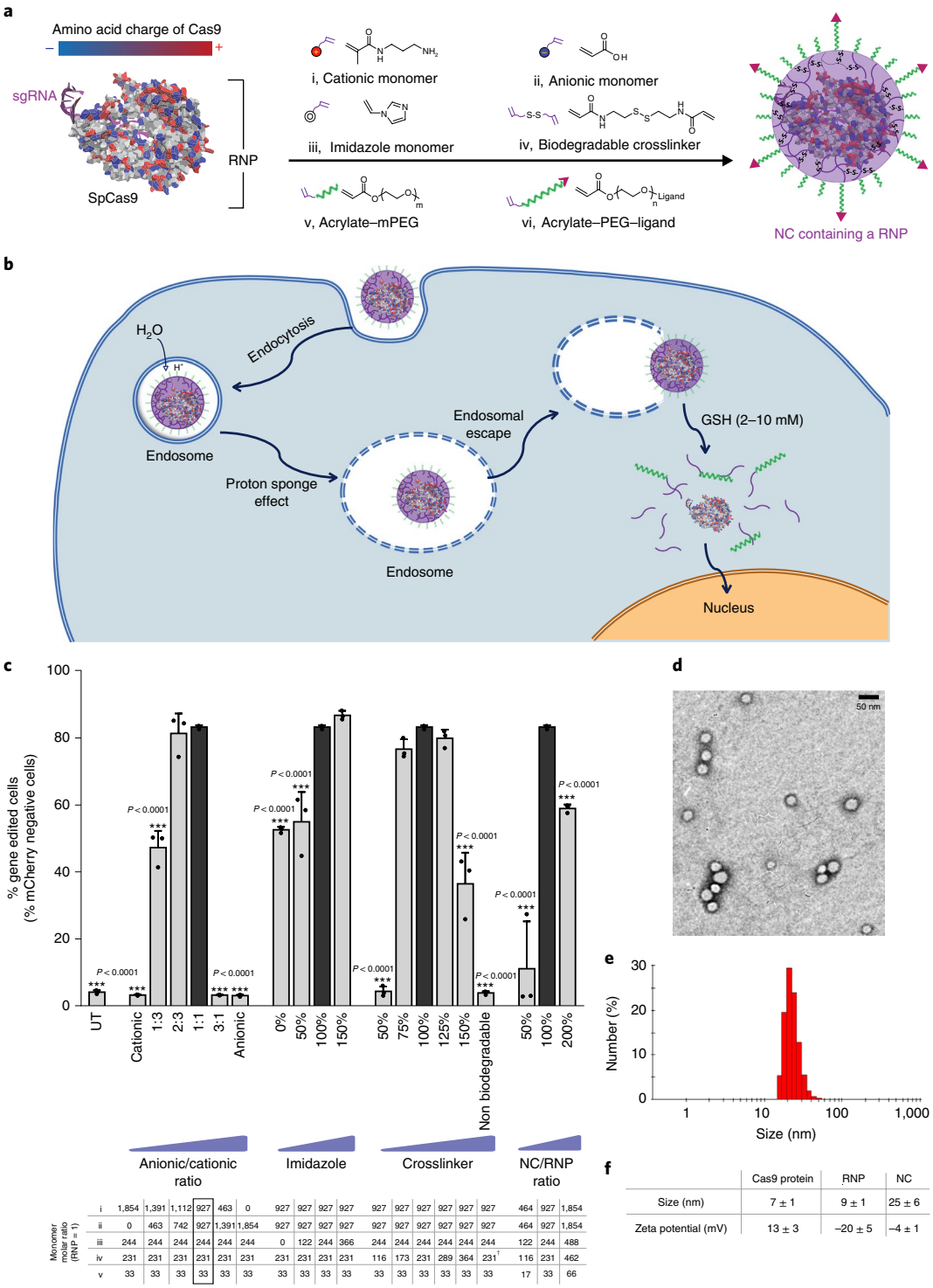

	Cas9 protein	RNP	NC
Size (nm)	7 ± 1	9 ± 1	25 ± 6
Zeta potential (mV)	13 ± 3	–20 ± 5	–4 ± 1

Fig. 1 | Design, synthesis and optimization of NCs. a, Streptococcus pyogenes Cas9 (SpCas9) has a heterogeneous surface charge due to both positive and negative amino acids residues, as well as the negatively charged sgRNA. A schematic illustration for the formation of the covalently crosslinked, yet intracellularly biodegradable, NC for the delivery of the Cas9 RNP complex prepared by in situ free-radical polymerization. **b**, A schematic depiction of the proposed mechanism of the cellular uptake of NCs and the subcellular release of the RNP. **c**, Optimizing the formulation of the NCs in vitro using mCherry-expressing HEK 293 (mCherry-HEK 293) cells. mCherry-HEK 293 cells were treated for six days with various formulations of the NCs with an sgRNA that targeted mCherry. The loss of mCherry fluorescence was measured by flow cytometry to assay the editing efficiency. The formulations investigated are listed in the bottom panel. The optimal NC formulation is highlighted by a black bar and its composition is shown by the black box below. To simplify reading the chart, the parameters being optimized (that is, anionic/cationic ratio, imidazole, crosslinker and NC/RNP ratio) are shown relative to the value of the same component in the optimal formulation. Data are presented as mean ± s.d. ($n = 3$). **d**, Transmission electron microscope image of NCs. A representative image is shown and experiments were repeated three times. **e**, Dynamic light scattering plots of NCs. A representative size distribution is shown and experiments were repeated three times. **f**, Summary of the size and zeta potential of Cas9 protein, Cas9 RNP and NC. Data are presented as mean ± s.d. ($n = 3$). Statistical significance was calculated via one-way analysis of variance (ANOVA) with a Tukey post hoc test. $^{*}P < 0.05$, $^{**}P < 0.01$, $^{***}P < 0.001$. †Non-biodegradable bisacrylamide.

(red fluorescence localized to each nucleus)[15,16]. Using a suitable sgRNA to target the mCherry transgene, successful gene editing results in a loss of red fluorescence that is easily detectable through flow cytometry.

It is essential to use both cationic and anionic monomers due to the heterogeneous charge distribution of the RNP (Fig. 1c). Pure cationic or anionic monomer formulations exhibited negligible gene editing, probably due to incomplete coating of the RNP. The ratios of anionic and cationic monomers also affected the gene editing efficiency. The formulation that contains a mixture of cationic and anionic monomers at an anionic/cationic ratio of 1:1 (the optimal formulation) exhibited the highest gene editing levels (Fig. 1c). The amounts of the imidazole monomer and biodegradable crosslinker were also critical for efficient gene editing (Fig. 1c). Without imidazole-containing monomers, NCs induced relatively low levels of gene editing. Higher editing efficiencies were achieved with increases in imidazole-containing monomers. Also, at a low crosslinker amount, no gene editing was observed, probably due to the unsuccessful formation of NCs. With sufficient amounts of crosslinker, similar gene editing capabilities were detected, which suggests a minimum required threshold for crosslinker to successfully form NCs. Higher crosslinker concentrations caused a reduction in gene editing efficiency. Furthermore, NCs formed by a non-biodegradable crosslinker (bisacrylamide) showed no editing, which indicates that NCs must be biodegradable to produce gene edits. The mass ratios between the NC and RNP impacted gene editing efficiencies, as sufficient monomers are needed to form a polymer coating around the RNP. NCs with a low NC/RNP ratio (50% of the optimal formulation) exhibited gene editing efficiencies barely above the baseline (Fig. 1c). However, excessive polymer coating over the RNP (200% of the optimal formulation) also reduced the editing efficiency, likely attributed to the fact that NCs with a thicker polymeric shell require a longer time to fully degrade and release the RNP to function. Collectively, the critical range for the functional encapsulation of RNPs was determined after systematically titrating all the key components, and the optimal NC formulation (hereafter referred to as NC) was selected for further study. The RNP loading level of the optimal NC was 40%. Figure 1d shows a transmission electron microscope image of uniformly sized NCs with an average diameter of 16 nm. The average hydrodynamic diameter of the NCs was 25 nm, as measured by dynamic light scattering (Fig. 1e). The zeta potential of the NCs was relatively neutral (that is, −4 mV), which indicates that the net negative charge of the RNP was masked by the NC (Fig. 1f).

The stability of the NCs before cell internalization is critical for successful genome editing. Although the GSH-degradable NCs are expected to remain stable in the extracellular spaces and circulation (GSH concentration, 0.001–0.02 mM)[12,13], their stability was systematically tested because the degradability of disulfide bonds in different polymers can differ[17]. To determine at which GSH concentration the NCs remain stable and functional, cell culture media that contained different concentrations of GSH were used during the NC treatment. The gene editing efficiency of the NCs did not change at a GSH concentration of 0.1 mM or lower, which indicates that the NCs were stable and functional at a GSH concentration at least up to 0.1 mM (Fig. 2a). At a GSH concentration of 1 mM or higher, the gene editing efficiency decreased, suggesting that NCs were disrupted before cell internalization. This also implies that NCs are GSH responsive and the RNP cargo can be efficiently released from NCs in the GSH-rich cytosol (2–10 mM).

We examined the subcellular localization of the RNP cargo in HEK 293 cells in vitro. As shown in Fig. 2b, after six hours of incubation, most of the RNP (red fluorescence) and endosomes (green fluorescence) were not overlapping, which indicates that RNPs were capable of escaping from the endosomes.

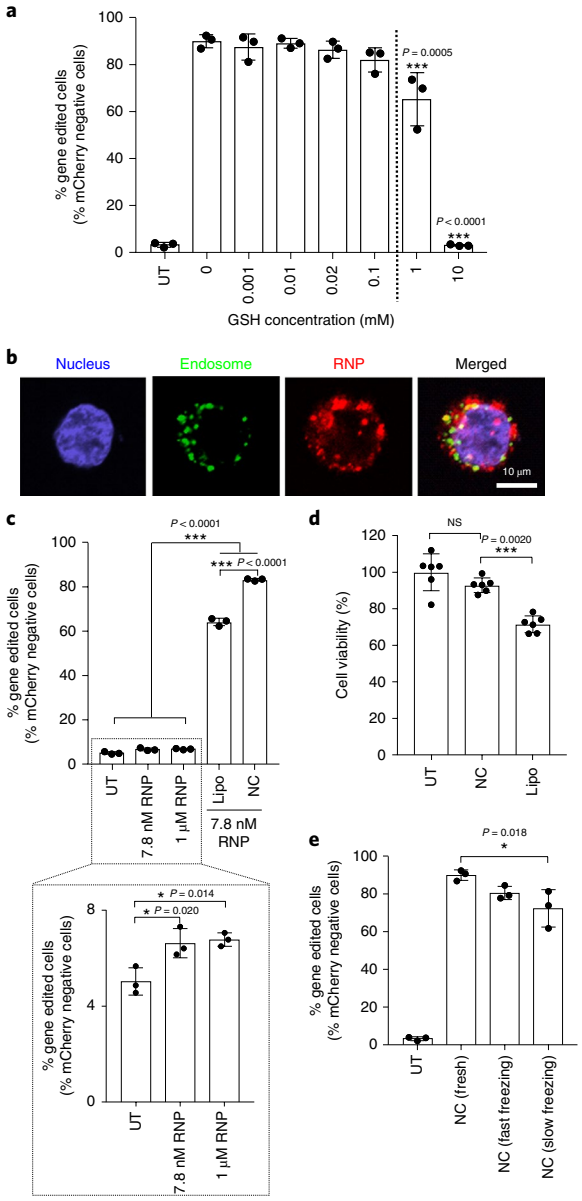

Fig. 2 | Stability, uptake and toxicity characteristics of NCs within human cells in vitro. a, Stability and responsiveness study of NCs with different concentrations of GSH. The gene editing efficiencies of NCs in GSH-containing media were tested in mCherry-HEK 293 cells with an sgRNA targeting mCherry. The loss of mCherry fluorescence was measured six days after transfection via flow cytometry to assay the editing efficiency. Data are presented as mean ± s.d. ($n = 3$). **b**, Intracellular distribution of NCs in HEK 293 cells using confocal laser scanning microscopy 6 h after transfection. The sgRNA was covalently labelled with the ATTO-550 fluorophore (red signal) to track its intracellular location. Cells were stained with LysoTracker Green DND-26 and DAPI (4,6-diamidino-2-phenylindole) for endosomes/lysosomes and nuclei, respectively. Experiments were repeated three times. **c**, Gene editing in mCherry-HEK 293 cells with unencapsulated RNP, optimized Lipo fectamine system (Lipo) or NCs. Data are presented as mean ± s.d. ($n = 3$). **d**, Cell viability measured by an MTT assay after treatment with Lipo and NCs. Data are presented as mean ± s.d. ($n = 6$). **e**, Editing efficiency of the NCs after lyophilization. Treatments included freshly prepared NCs (NC (fresh)), NCs lyophilized after a fast freezing process (NC (fast freezing)), or NCs lyophilized after a slow freezing process (NC (slow freezing)). Data are presented as mean ± s.d. ($n = 3$). Statistical significance was calculated via one-way ANOVA with a Tukey post hoc test. $^{*}P < 0.05$, $^{**}P < 0.01$, $^{***}P < 0.001$. NS, not significant.

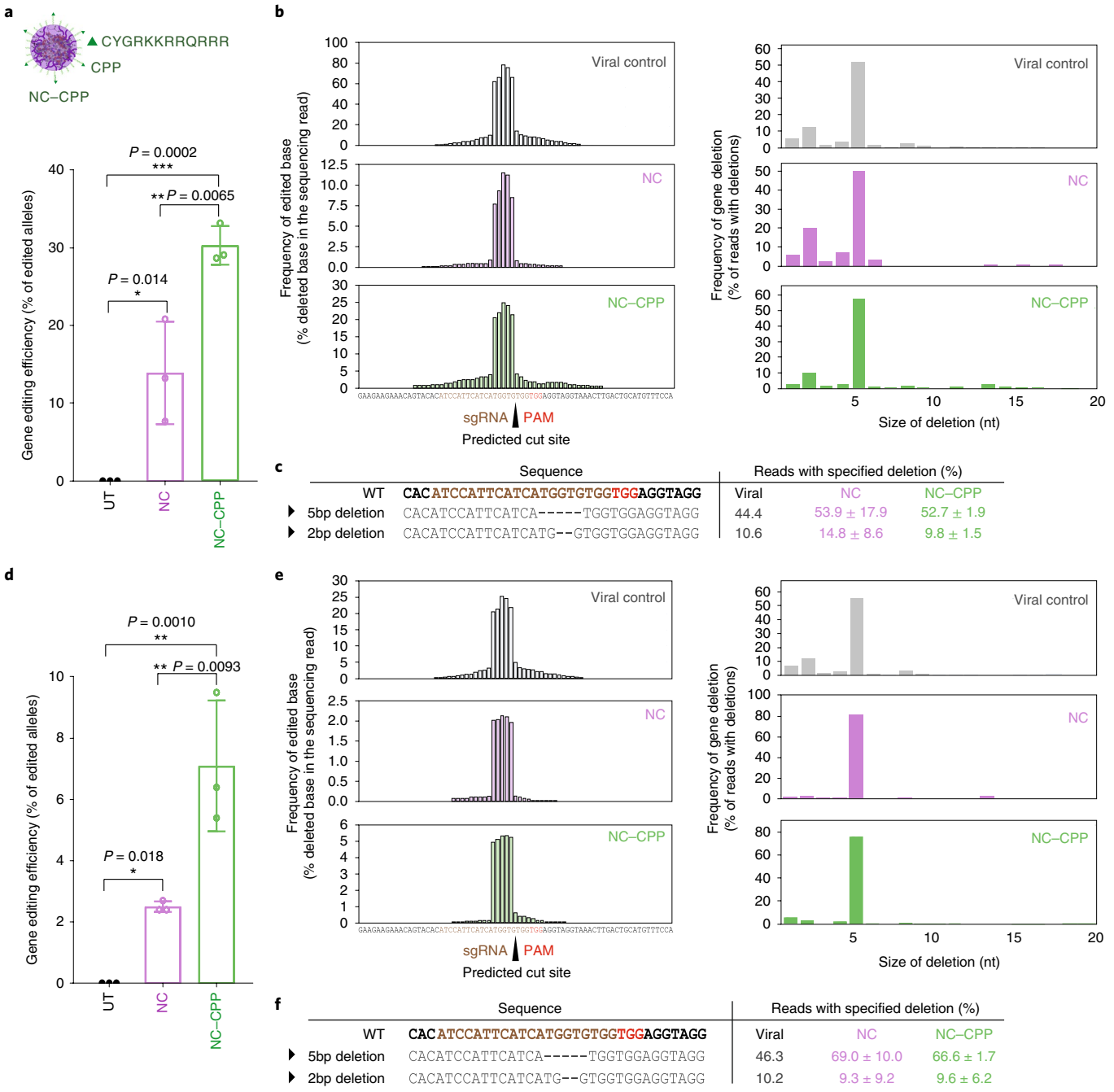

Fig. 3 | Decoration of NCs with cell penetrating peptides increases on-target genome editing efficiency in vitro within human cell lines. a, Deep sequencing of HEK 293 cells transfected with an NC that contains a Cas9 RNP with an sgRNA that targets the endogenous *APP* locus. NCs were decorated with CPPs (NC–CPP) (top). Targeted PCR amplification around the on-target site revealed high on-target editing by NCs. The percentage of sequencing reads with a genomic edit is plotted compared to an untransfected control sample (UT). Data are presented as mean ± s.d. ($n = 3$). **b**, Deletion spectra (left column) for reads with deleted bases are shown for every base proximal to the sgRNA target. Viral control refers to previously characterized spectrum for this sgRNA in HEK 293 cells from Sun et al.[21] The right column shows the size of deletions in the edited sequencing reads. **c**, Frequencies of major reads with deletions in HEK 293 cells. Data are presented as mean ± s.d. ($n = 3$). **d**, Deep sequencing of hESCs transfected with an NC that contains a Cas9 RNP with an sgRNA that targets the endogenous *APP* locus. Data are presented as mean ± s.d. ($n = 3$). **e**, Deletion spectra (left column) and size of deletions (right column) in hESCs as noted in **b**. **f**, Frequencies of major reads with deletions in hESCs. Data are presented as mean ± s.d. ($n = 3$). Statistical significance was calculated via one-way ANOVA with a Tukey post hoc test. $^*P < 0.05$, $^{**}P < 0.01$, $^{***}P < 0.001$. PAM, protospacer adjacent motif; nt, nucleotide.

We then compared the in vitro gene editing functionality of NCs with Lipofectamine-based delivery vehicles (for example, Lipofectamine 2000 (Lipo) and Lipofectamine CRISPRMAX); state-of-the-art, commercially available transfection agents for RNP delivery. Lipofectamine delivery systems were also systemically optimized (Supplementary Fig. 1); Lipo with 0.75 µl per well in the 96-well plate exhibited the highest gene editing efficiency, which was used for the subsequent study. Unencapsulated RNP treatment was included as the RNP itself shows some cell penetrating capability, probably conferred by the positively charged NLSs[18]. Compared

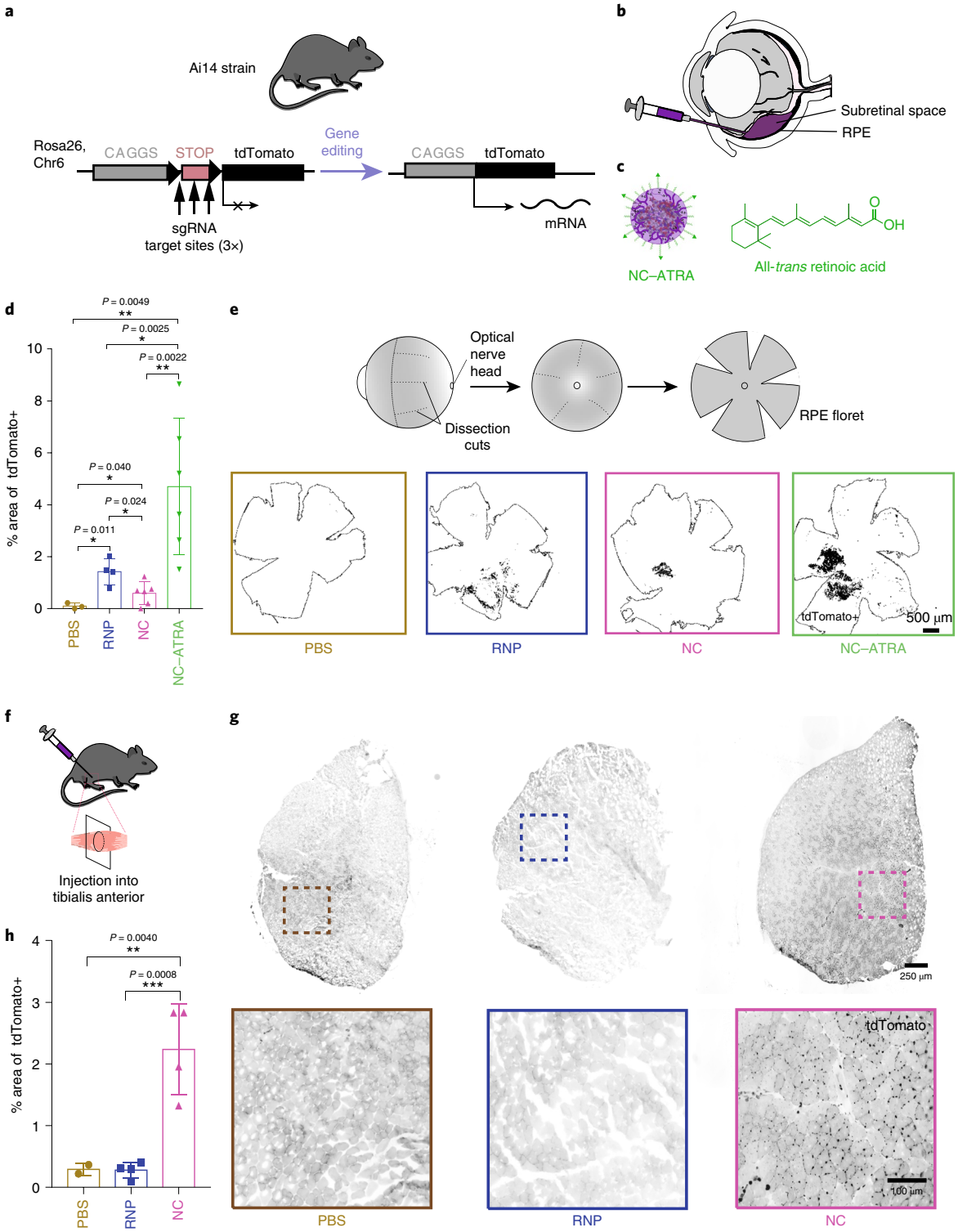

Fig. 4 | NCs can induce efficient genome editing in vivo within Ai14 reporter mice. a, Schematic of the tdTomato locus within the Ai14 mouse strain. A STOP cassette that consists of three SV40 polyA sequences prevents transcription of the downstream red fluorescent protein variant, tdTomato (left). When cells are edited by CRISPR/Cas9 to excise the STOP cassette via cut sites present in each of the repeats, they express tdTomato (right). **b**, Schematic of the subretinal injection of genome editors to target the RPE cells. **c**, Illustration of NC–ATRA. **d**, Genome editing efficiency as quantified by the percentage area of whole RPE with the genome editing reporter (tdTomato+). PBS ($n=3$), RNP ($n=4$), NC ($n=6$) or NC–ATRA ($n=6$). Data are presented as mean ± s.d. **e**, Schematic of whole-mount RPE preparation (top) and representative images of the tdTomato+ signal (black) 12 days after the subretinal injection (bottom). The whole RPE layer is outlined. Experiments were repeated three times. **f**, Schematic of the intramuscular injection of genome editors. **g**, Representative images of the muscle tissues 12 days after the intramuscular injection of PBS, RNP or NC: the confocal fluorescent signal for tdTomato is shown in black. Experiments were repeated three times. **h**, Gene editing efficiency as quantified by the percentage area of whole-muscle tissue with a genome editing reporter (tdTomato+). $n=4$ for all the conditions except PBS ($n=2$). Data are presented as mean ± s.d. Statistical significance was calculated via one-way ANOVA with a Tukey post hoc test. $^{*}P<0.05$, $^{**}P<0.01$, $^{***}P<0.001$.

to the untreated control, RNP alone induced only 1.6 ± 0.5% editing above the background levels, which was significantly lower than that delivered by either Lipo (60.1 ± 1.7%) or NC (79.1 ± 0.6%), where NCs exhibited the highest editing efficiency (Fig. 2c). Moreover, NCs did not cause apparent cytotoxicity in HEK 293 cells (<6% cell death), whereas, consistent with other studies, Lipo exhibited significant cytotoxicity when it was used to deliver the same amount of RNP (~25% cell death (Fig. 2d)). Importantly, the NCs can be freeze-dried and reconstituted at high concentrations (~5 μg μl^{-1}RNP) while retaining potency (>90%), unlike many liposomal delivery agents that lose stability on freeze-drying[19] (Fig. 2e).

To demonstrate the versatility of NC surface modification, we first functionalized NCs with CPPs (that is, NC–CPP (Fig. 3a)), which are known to enhance the cellular uptake efficiency of nanoparticles. CPPs (or the targeting ligand, all-*trans* retinoic acid (ATRA), used in the subsequent in vivo experiments) were incorporated onto the distal ends of a higher molecular weight 2 kDa PEG. The use of longer PEGs could potentially reduce the steric hindrance from the surrounding 480 Da mPEG segments, which allows for better targeting or penetrating capabilities[20]. Detailed polymer and NC characterizations are shown in the Supplementary Information (Supplementary Figs. 2 and 3 and Supplementary Table 1). As expected, CPP conjugation on NCs significantly enhanced (~1.5-fold) their level of cellular uptake (Supplementary Fig. 4). Moreover, when loaded with RNP that targets the endogenous *APP* gene, NC–CPP enhanced the editing efficiency in HEK 293 cells as well as human embryonic stem cells (hESCs), a notoriously hard-to-transfect cell type (Fig. 3). Deep sequencing of the on-target region around *APP* revealed high-efficiency editing at this endogenous locus. In HEK 293 cells, NC–CPP increased the editing efficiency twofold (Fig. 3a), whereas in hESCs, NC–CPP increased the editing efficiency approximately threefold (Fig. 3d). The deletion spectra (Fig. 3b–e) for both cell types contained a 5 base deletion as a frequent editing outcome in all the samples, consistent with a previous report using this sgRNA sequence[21]. Together, these in vitro results demonstrate that decoration of the NC can enhance genome editing at an endogenous, therapeutically relevant locus without changing the types of edits produced by Cas9.

Gene editing using NCs was finally evaluated in vivo in the eyes and muscles of transgenic Ai14 mice (Fig. 4). All cells within Ai14 mice contain a stop cassette that comprises three sv40 polyA transcription terminators, which prevent the expression of a constitutive tdTomato fluorescent reporter. tdTomato expression can be induced via excision of the sv40 polyA genetic elements (Fig. 4a). Successful gene editing can therefore be easily evaluated through fluorescence[18]. First, we evaluated gene editing within the retinal pigment epithelium (RPE) because over two million people worldwide are affected by monogenic diseases of the eye[22], and several somatic gene editing strategies are being developed for subretinal delivery[23]. We tested whether surface modification of the NC could affect its gene editing performance within RPE. NCs were decorated with ATRA (NC–ATRA). ATRA binds to the interphotoreceptor retinoid-binding protein, a major protein in the interphotoreceptor matrix that selectively transports 11-*cis*-retinal to the photoreceptor outer segments and all-*trans*-retinol to the RPE[24]. Mice were subretinally injected with a PBS vehicle, RNP alone, NC or NC–ATRA (Fig. 4b,c). A successful subretinal injection was indicated by a bleb formation immediately next to the RPE (Supplementary Fig. 5). At 12 days postinjection, the enucleated eyes were whole mounted to evaluate the gene editing globally over the entire RPE tissue (Fig. 4d,e). In contrast to the in vitro results in HEK 293 cells discussed above and the in vivo results in muscle cells discussed below, where RNP alone did not induce any genome editing, the unencapsulated RNP was able to induce genome editing in RPE cells. This may be attributed to the inherent function of this tissue as a transport epithelium: RPE cells are involved in the movement of nutrients and waste products through bidirectional passive and active pathways[25,26]. The subretinal space is a tight space that ensures fluid absorption from the retina to the choroid direction through the RPE layer for retina reattachment after subretinal injections, and RPE cells are among the most actively phagocytic cells found in the body[27,28]. NCs also exhibited considerable gene editing, and NC–ATRA induced a significantly higher editing efficiency than other groups (Fig. 4d,e). Second, we tested the activity of NCs in muscle tissue via intramuscular administration in the same mouse model (Fig. 4f). As shown in Fig. 4g,h, unencapsulated RNP failed to induce any genome editing in muscles, whereas NCs induced robust gene editing. Interestingly, strong tdTomato signals were identified in the cells within the basal lamina between muscle fibres. As muscle satellite cells—quiescent mononucleated myogenic cells in adult muscle—are present in this region, we performed immunohistochemistry to co-stain with Pax7 (a muscle satellite cell marker) and tdTomato (RFP) in the muscle sections. Overlapping signals of Pax7 and RFP in the NC-injected muscle (Supplementary Fig. 6) indicated that Pax7-positive satellite cells expressed tdTomato protein. Collectively, these results demonstrated that NC formulations could produce gene edits in vivo, the extent of which can be further modulated by surface functionalization.

Our approach accommodates the charge heterogeneity of Cas9 RNP (~9 nm in diameter) to form covalently linked stable, yet biodegradable, NCs. NCs were formed by coating RNPs using a mixture of monomers with distinct functions, as described above. The RNP serves as the core or scaffold for the formation of the NC. The monomers are attracted to the RNP surface either electrostatically or via van der Waals forces and hydrogen bonding for subsequent polymerization, which results in nearly monodispersed NCs with an average size of 16 nm in the dried state. This chemically defined strategy, therefore, has a fixed stoichiometry between the NC and RNP that constitutes a predictable formulation considerably smaller than those of other non-viral Cas9 delivery strategies.

The monomeric precursors of NCs allow for easy fine-tuning of the ratios and amounts of monomers to control the endosomal escape and cytosol release of RNP from NCs, as well as the conjugation of functional moieties. This customizability is a key advantage over methods based on lipids[29] and protein engineering[30], which may be less flexible. NCs also retain their biological functions after freeze-drying, and thereby allow for long-term storage and transport. Furthermore, employing protein engineering to facilitate delivery may alter Cas9–sgRNA interactions and interfere with proper RNP function, as described previously[30]. Our NC delivery system demonstrated robust gene editing outcomes and lower cytotoxicity. Finally, the NC delivery system also induced efficient gene editing in vivo, which highlights its versatility via surface modification. Owing to the small size, modularity and low cytotoxicity of NCs, we anticipate that they could be further tailored to efficiently deliver gene editing machinery to a multitude of cell lines in vitro and many tissues in vivo for somatic gene editing applications.

Online content

Any methods, additional references, Nature Research reporting summaries, source data, statements of code and data availability and associated accession codes are available at https://doi.org/10.1038/s41565-019-0539-2.

Received: 6 December 2017; Accepted: 26 July 2019;
Published online: 9 September 2019

References

1. Yin, H., Kauffman, K. J. & Anderson, D. G. Delivery technologies for genome editing. *Nat. Rev. Drug Discov.* **16**, 387–399 (2017).
2. Liu, J. et al. Efficient delivery of nuclease proteins for genome editing in human stem cells and primary cells. *Nat. Protocols* **10**, 1842–1859 (2015).

3. Li, L., He, Z., Wei, X., Gao, G. & Wei, Y. Challenges in CRISPR/CAS9 delivery: potential roles of nonviral vectors. *Hum. Gene Ther.* **26**, 452–462 (2015).
4. Mout, R., Ray, M., Lee, Y. W., Scaletti, F. & Rotello, V. M. In vivo delivery of CRISPR/Cas9 for therapeutic gene editing: progress and challenges. *Bioconjugate Chem.* **28**, 880–884 (2017).
5. Wang, H. X. et al. CRISPR/Cas9-based genome editing for disease modeling and therapy: challenges and opportunities for nonviral delivery. *Chem. Rev.* **117**, 9874–9906 (2017).
6. Li, L., Hu, S. & Chen, X. Non-viral delivery systems for CRISPR/Cas9-based genome editing: challenges and opportunities. *Biomaterials* **171**, 207–218 (2018).
7. Rui, Y., Wilson, D. R. & Green, J. J. Non-viral delivery to enable genome editing. *Trends Biotechnol.* **37**, 281–293 (2019).
8. Gu, Z. et al. Protein nanocapsule weaved with enzymatically degradable polymeric network. *Nano Lett.* **9**, 4533–4538 (2009).
9. Zhao, M. et al. Clickable protein nanocapsules for targeted delivery of recombinant p53 protein. *J. Am. Chem. Soc.* **136**, 15319–15325 (2014).
10. Yan, M. et al. A novel intracellular protein delivery platform based on single-protein nanocapsules. *Nat. Nanotechnol.* **5**, 48–53 (2010).
11. Putnam, D., Gentry, C. A., Pack, D. W. & Langer, R. Polymer-based gene delivery with low cytotoxicity by a unique balance of side-chain termini. *Proc. Natl Acad. Sci. USA* **98**, 1200–1205 (2001).
12. Meng, F., Cheng, R., Deng, C. & Zhong, Z. Intracellular drug release nanosystems. *Mater. Today* **15**, 436–442 (2012).
13. Liu, F. et al. PKM2 methylation by CARM1 activates aerobic glycolysis to promote tumorigenesis. *Nat. Cell Biol.* **19**, 1358–1370 (2017).
14. Mout, R. et al. Direct cytosolic delivery of CRISPR/Cas9-ribonucleoprotein for efficient gene editing. *ACS Nano* **11**, 2452–2458 (2017).
15. Carlson-Stevermer, J. et al. High-content analysis of CRISPR-Cas9 gene-edited human embryonic stem cells. *Stem Cell Rep.* **6**, 109–120 (2016).
16. Carlson-Stevermer, J. et al. Assembly of CRISPR ribonucleoproteins with biotinylated oligonucleotides via an RNA aptamer for precise gene editing. *Nat. Commun.* **8**, 1711 (2017).
17. Elzes, M. R., Akeroyd, N., Engbersen, J. F. & Paulusse, J. M. Disulfide-functional poly(amido amine)s with tunable degradability for gene delivery. *J. Control. Release* **244**, 357–365 (2016).
18. Staahl, B. T. et al. Efficient genome editing in the mouse brain by local delivery of engineered Cas9 ribonucleoprotein complexes. *Nat. Biotechnol.* **35**, 431–434 (2017).
19. Payton, N. M., Wempe, M. F., Xu, Y. & Anchordoquy, T. J. Long-term storage of lyophilized liposomal formulations. *J. Pharm. Sci.* **103**, 3869–3878 (2014).
20. Chen, G. et al. Multi-functional self-fluorescent unimolecular micelles for tumor-targeted drug delivery and bioimaging. *Biomaterials* **47**, 41–50 (2015).
21. Sun, J. et al. CRISPR/Cas9 editing of APP C-terminus attenuates β-cleavage and promotes α-cleavage. *Nat. Commun.* **10**, 53 (2019).
22. Berger, W., Kloeckener-Gruissem, B. & Neidhardt, J. The molecular basis of human retinal and vitreoretinal diseases. *Prog. Retin. Eye Res.* **29**, 335–375 (2010).
23. Maeder, M. L. et al. Development of a gene-editing approach to restore vision loss in Leber congenital amaurosis type 10. *Nat. Med.* **25**, 229–233 (2019).
24. Sun, D. et al. Targeted multifunctional lipid ECO plasmid DNA nanoparticles as efficient non-viral gene therapy for Leber's congenital amaurosis. *Mol. Ther. Nucleic Acids* **7**, 42–52 (2017).
25. Marmor, M. F. Control of subretinal fluid: experimental and clinical studies. *Eye* **4**, 340–344 (1990).
26. Strauss, O. The retinal pigment epithelium in visual function. *Physiol. Rev.* **85**, 845–881 (2005).
27. Mao, Y. & Finnemann, S. C. in *Retinal Degeneration* (eds Weber, B. & Langmann, T.) 285–295 (Springer, 2012).
28. Mazzoni, F., Mao, Y. & Finnemann, S. C. in *Retinal Degeneration* (eds Weber, B. & Langmann, T.) 95–108 (Springer, 2019).
29. Steyer, B. et al. High content analysis platform for optimization of lipid mediated CRISPR-Cas9 delivery strategies in human cells. *Acta Biomater.* **34**, 143–158 (2016).
30. Zuris, J. A. et al. Cationic lipid-mediated delivery of proteins enables efficient protein-based genome editing in vitro and in vivo. *Nat. Biotechnol.* **33**, 73–80 (2015).

Acknowledgements

We thank the James Thomson lab for the use of their BD FACSCanto II, and the University of Wisconsin Biotechnology Center for providing facilities and services. We thank Aldevron for supplying reagents and technical support. We are grateful to Q. Chang who provided us with the Ai14 tdTomato transgenic mice used for the initial evaluation. We acknowledge the generous financial support from the National Institute for Health (1-UG3-NS-111688-01, R01EY024995, 1R35GM119644, R01NS091540, R01HL143469 and R01 HL129785), the National Science Foundation (CBET-1350178 and CBET-1645123), the Wisconsin Alumni Research Foundation and the Wisconsin Institute for Discovery. The authors also acknowledge financial support from the University of Wisconsin–Madison.

Author contributions

G.C., A.A.A., Y.W., K.S. and S.G. conceived and designed the project, G.C., A.A.A., Y.W., R.X., M.S., S.R. and P.K.S. performed the experiments, all the authors analysed the data and G.C., A.A.A., Y.W., P.K.S., B.R.P., M.S., K.S. and S.G. co-wrote the paper.

Competing interests

G.C., A.A.A., Y.W., R.X., K.S. and S.G. have filed a patent application on this work.

Additional information

Supplementary information is available for this paper at https://doi.org/10.1038/s41565-019-0539-2.

Reprints and permissions information is available at www.nature.com/reprints.

Correspondence and requests for materials should be addressed to K.S. or S.G.

Publisher's note: Springer Nature remains neutral with regard to jurisdictional claims in published maps and institutional affiliations.

Methods

Materials. Acrylic acid (AA), *N*,*N*,*N*′,*N*′-tetramethylethylenediamine (TMEDA), acrylate PEG (APEG) (480 Da), bisacrylamide, 1-vinylimidazole (VI) and ammonium persulfate (APS) were purchased from ThermoFisher Scientific. APEG–NH_2 (2 kDa) was acquired from JenKem Technology. ATRA, *N*-(3-aminopropyl) methacrylamide hydrochloride (APMA) and BACA were obtained from Sigma-Aldrich. APEG–Mal (2 kDa) was purchased from Creative PEGWorks. The CPP, Cys-TAT (CYGRKKRRQRRR), was synthesized by Genscript. Lipofectamine 2000 and CRISPRMax were purchased from ThermoFisher Scientific.

Cell culture. The HEK 293 cell line was maintained on gelatin-A coated plates at passage 10–50 in DMEM supplemented with 10% FBS, 2 mM L-glutamine, and 50 U mL^{-1} penicillin/streptomycin. WA09 hESCs were maintained in mTESR medium on Matrigel (WiCell)-coated tissue culture polystyrene plates. hESCs were passaged every 3–4 days at a 1:6 ratio using Versene solution (Life Technologies). H2B-mCherry transgenic lines were generated as previously reported[31] through the CRISPR-mediated insertion of an AAV-CAGGS-EGFP plasmid (Addgene no. 22212), modified to express histone 2B-mCherry, at the *AAVS1* safe harbour locus using gRNA AAVS1-T2 (Addgene no. 41818). All the cells were maintained at 37 °C and 5% CO_2. Cell lines were kept mCherry positive through puromycin selection or fluorescence-assisted cell sorting (FACS) on a BD FACS Aria.

sgRNAs in vitro transcription. A DNA double-stranded template of a truncated T7 promoter and desired sgRNA sequence was formed through overlap PCR using Q5 high-fidelity polymerase (New England Biolabs) according to the manufacturer's protocols and was placed in the thermocycler for 35 cycles of 98 °C for 5 s, 52 °C for 10 s and 72 °C for 15 s, with a final extension period of 72 °C for 10 min. PCR products were then incubated overnight at 37 °C in a HiScribe T7 in vitro transcription reaction (New England Biolabs) according to the manufacturer's protocol. The resulting RNA was purified using a MEGAclear Transcription Clean-Up Kit (Thermo Fisher). The sgRNA concentration was quantified using a Qubit fluorometer (Thermo Fisher). The sgRNA sequences used were (with the protospacer adjacent motif site): mCherry: GGAGCCGTACATGAACTGAGGGG, APP: ATCCATTCATCATGGTGTGGTGG and the stop cassette before tdTomato (Ai14): AAGTAAAACCTCTACAAATGTGG.

Preparation of NCs. Sodium bicarbonate buffer (10 mM, pH = 9.0) was freshly prepared and degassed using the freeze–pump–thaw method for three cycles. The sNLS-Cas9-sNLS protein (Aldevron) was combined with sgRNA at a 1:1 molar ratio and allowed to complex for 5 min with gentle mixing. AA, APMA, VI and APEG were accurately weighed and dissolved in degassed sodium bicarbonate buffer (2 mg ml^{-1}). APS and TMEDA were accurately weighed and dissolved in degassed sodium bicarbonate buffer (1 mg ml^{-1}). The Cas9 RNP complex was diluted to 0.12 mg ml^{-1} in sodium bicarbonate buffer in a nitrogen atmosphere. Monomer solutions were added into the above solution under stirring in the order of AA, APMA and VI at 5 min intervals. In each 5 min interval, the solution was degassed by vacuum pump for 3 min and refluxed with nitrogen. After another 5 min, the crosslinker, BACA, was added, followed by the addition of APS. The mixture was degassed for 5 min, and the polymerization reaction was immediately initiated by the addition of TMEDA. After 65 min of polymerization under a nitrogen atmosphere, the APEG was added. The reaction was resumed for another 30 min. Finally, unreacted monomers and initiators were removed by dialysis in 20 mM PBS buffer (pH 7.4). The molar ratio of AA/APMA/VI/BACA/APEG (i/ii/iii/iv/v) used for the optimal formulation was 927/927/244/231/33. The molar ratio of RNP/APS/TMEDA was kept at 1/1/1.

For the preparation of NCs conjugated with CPP (that is, NC–CPP), we first prepared APEG–CPP by reacting APEG–Mal and Cys-TAT through a sulfhydryl–Mal reaction in an aqueous solution at a pH of 7.4. Then, the NC–CPP was prepared following a similar protocol to that described above with the molar ratio of AA/APMA/VI/BACA/APEG-CPP at 927/927/244/231/33.

For the preparation of NC–ATRA, APEG–ATRA was first prepared by reacting APEG-NH_2 and ATRA through amidization. Briefly, APEG–NH_2 (0.1 mmol), ATRA (0.12 mmol), 1-ethyl-3-(3-dimethylaminopropyl)carbodiimide (0.12 mmol) and *N*-hydroxysuccinimide (0.15 mmol) were dissolved in DMSO (5 mL). The solution was stirred at room temperature for 24 h. Subsequently, it was dialysed against deionized water for 48 h to remove impurities. The polymer APEG–ATRA was obtained by lyophilization (Labconco). Then, the NC–ATRA was prepared following a similar protocol to that described above with the molar ratio of AA/APMA/VI/BACA/APEG/APEG-ATRA at 927/927/244/231/33.

The dried NCs were prepared using either a fast or slow freezing process before lyophilization. For the fast freezing process, NC solutions were frozen rapidly using liquid nitrogen and were then dried using a lyophilizer. For the slow freezing process, NC solutions were frozen using a Mr Frosty freezing container at a cooling rate of −1 °C min^{-1} (Thermo Fisher Scientific) and were then dried using a lyophilizer.

Characterization. The sizes and morphologies of Cas9 RNP NCs were studied by dynamic light scattering (ZetaSizer Nano ZS90) and transmission electron microscopy (FEI Tecnai 12, 120 keV). Zeta potentials were measured by a ZetaSizer Nano ZS90 (Malvern Instruments). The RNP loading level of the NCs were determined by the bicinchoninic acid assay.

Assaying RNP delivery. Cells were seeded in 96-well plates in 100 µl of media one day prior to transfection. On the day of transfection, unencapsulated RNP, NC-RNP or Lipofectamine-based RNP complexes (including Lipofectamine 2000/RNP and Lipofectamine CRISPRMAX/RNP) were added to the cells for transfection of RNPs according to manufacturer instructions (for example, 0.2–0.75 µl per well of Lipofectamine 2000 and 0.3 µl per well of Lipofectamine CRISPRMAX). At day 6, cells were collected for flow cytometry (BD FACSCanto II) and assayed for mCherry expression. Flow analysis was performed using FlowJo software. For HEK 293 cells, 7.8 nM RNP was used per well. To examine the activity of unencapsulated RNP, a high dose (1 µM) of RNP was also tested.

For experiments that involved *APP* targeting, cells were cultured in 24 well plates at 50,000 cells per well. HEK 293 cells were transfected with 6.25 nM RNP, whereas 25 nM RNP was used to transfect hESCs.

To study the stability of the RNP NCs in the presence of GSH, the gene editing efficiency of the NCs under different GSH concentrations was tested. The experiments were carried out under similar conditions to those described above, but using GSH-containing media instead. The GSH concentration investigated ranged from 0 to 10 mM.

Genomic analysis. DNA was isolated from cells using DNA QuickExtract (Lucigen) after treatment with 0.05% trypsin-EDTA and centrifugation. The QuickExtract solution was incubated at 65 °C for 15 min, 68 °C for 15 min and then 98 °C for 10 min. Genomic PCR was performed following the manufacturer's instructions using a Q5 High fidelity DNA polymerase (New England Biolabs) and ~500 ng of genomic DNA. Products were then purified using AMPure XP magnetic bead purification kit (Beckman Coulter) and quantified using a Nanodrop2000 or Qubit (Thermo Fisher). For deep sequencing of the *APP* locus, genomic DNA was amplified using the primers (5′ to 3′) TGTCATAGCGACAGTGATCGT and AGCTAAGCCTAATTCTCTCATAGTC. Samples were pooled and run on an Illumina Miniseq with a read length of 150 bp. Deep sequencing data were analysed using the Cas-Analyzer software[32].

Intracellular trafficking. HEK 293 cells were seeded at a density of ~40,000 cells per well one day prior to transfection in 1 µm 2-well culture chambers (Ibidi). NCs were formed with Atto-550 fluorescently tagged *trans*-activating CRISPR RNA (Integrated DNA Technologies) combined with CRISPR RNA and added to cells at 1 µg per well for transfection. After 6 h of incubation, cells were stained with LysoTracker Green DND-26 and DAPI for endosomes/lysosomes and nuclei, respectively. Cells were imaged using an Eclipse TI epifluorescent microscope (Nikon) and an AR1 confocal microscope (Nikon). For the flow cytometric analysis, HEK 293 cells were seeded in 96 well plates and dissociated after 4 h, followed by flow cytometry on an Accuri C6 (BD Biosciences).

MTT assay. HEK 293 cells were seeded in 96-well plates (17,500 cells per well) in 100 µl of media 1 day prior to transfection. On the day of transfection, NC, RNP and Lipo (0.2–0.75 µl per well) or RNP and Lipofectamine CRISPRMAX (0.3 µl per well) were added to the cells. After 2 days of incubation, a standard MTT assay was performed by aspirating the treatment media, adding 100 µl of the medium that contained 0.5 mg ml^{-1} MTT agent and incubating at 37 °C for 4 h. Thereafter, the medium was aspirated and 75 µl of dimethylsulfoxide was added to each well. The plates were then measured at 570 nm using a spectrophotometer (Quant, Bio-Tek Instruments) and the average absorbance and percentage of cell viability relative to the control (pure medium) were calculated.

Subretinal Injection. For mice studies, Ai14 mice (obtained from Jackson Labs) were used to assay the gene editing efficiency in RPE. All the RNPs were formed with sgRNA targeted for the excision of SV40 polyA blocks[22]. As previously described, mice were maintained under a tightly controlled temperature (23 ± 5 °C), humidity (40–50%) and light/dark (12/12 h) cycle conditions in a 200 lux light environment. The mice were anaesthetized by intraperitoneal injection of a ketamine (80 mg kg^{-1}), xylazine (16 mg kg^{-1}) and acepromazine (5 mg kg^{-1}) cocktail. Prior to the subretinal injection, the cornea was anaesthetized with a drop of 0.5% proparacaine HCl and the pupil was dilated with 1.0% tropicamide ophthalmic solution (Bausch & Lomb Inc.). Thermal stability was maintained by placing mice on a temperature-regulated heating pad during the injection and for recovery purposes. All the surgical manipulations were carried out under a surgical microscope (AmScope). A solution (2 µl) that contained RNP alone, NC or NC–ATRA at a concentration of 8 µg Cas9 was injected into the subretinal space using the UMP3 ultramicropump fitted with a NanoFil syringe and the RPE-KIT (all from World Precision Instruments) equipped with a 34-gauge bevelled needle. Successful administration was confirmed by bleb formation (Supplementary Fig. 5). The tip of the needle remained in the bleb for 10 s after bleb formation, after which it was gently withdrawn. A solution (2 µl) of the PBS vehicle was also injected into the subretinal space of the contralateral eye to serve as a control.

To assess the tdTomato expression generated by successful gene editing, the mice were euthanized and eyes were collected 12 days after injection. Enucleated eyes from these mice were rinsed twice with PBS, a puncture was made at ora serrata with an 18-gauge needle and the eyes were opened along the corneal incisions. The lens was then carefully removed. The eye cup was flattened, making incisions radially to the centre, to give the final 'starfish' appearance. The retina was then separated gently from the RPE layer. The separated RPE and retina were flat mounted on the cover-glass slide and imaged with NIS-Elements using a Nikon C2 confocal microscope (Nikon Instruments Inc.). A diode laser (561 nm) for red excitation was used to evaluate the tdTomato expression in the RPE layer and images were captured by Low Noise PMT C2 detectors in a Plan Apo VC ×20/0.75, 1 mm WD lens. ImageJ (NIH) was used for image analysis to measure the tdTomato positive areas in relevant regions of interest (masked to RPE areas from brightfield images).

Intramuscular injection. All treatments (PBS, RNP and NC) were administered to adult mice via the tibialis anterior (TA, 8–10 µl per muscle) using a 33-gauge needle with a Hamilton syringe. TA muscles were harvested and flash-frozen in super-cooled isopentane 12 days postinjection and then sectioned at 20 µm using a cryostat and placed on glass slides. After mounting on a slide glass, muscle sections were observed by using a Keyence BZ-X710 fluorescence microscope (Osaka) to visualize the tdTomato fluorescence. For quantification of the fluorescence signals, three sections per muscle were selected from the similar locations in the TA muscle. The relative intensity of tdTomato-positive signal was densitometrically evaluated using NIH ImageJ software.

For immunohistochemistry, the muscle sections were fixed with 4% paraformaldehyde–PBS, and then incubated with primary antibodies overnight. The primary antibodies used to probe for muscle satellite cells and tdTomato were, respectively, anti-Pax7 (Developmental Studies Hybridoma Bank) and anti-RFP (rabbit polyclonal, Rockland Immunochemical Inc.). The primary antibodies were then detected by fluorescence-conjugated secondary antibodies. All the images were acquired using a Nikon Eclipse 80i fluorescence microscope with a digital camera (DS-QiIMC, Nikon).

Reporting summary. Further information on research design is available in the Nature Research Reporting Summary linked to this article.

Data availability

The data that support the plots within this paper and other findings of this study are available from the corresponding authors upon reasonable request.

References

31. Harkness, T. et al. High-content imaging with micropatterned multiwell plates reveals influence of cell geometry and cytoskeleton on chromatin dynamics. *Biotechnol. J.* **10**, 1555–1567 (2015).
32. Park, J., Lim, K., Kim, J. S. & Bae, S. Cas-analyzer: an online tool for assessing genome editing results using NGS data. *Bioinformatics* **33**, 286–288 (2017).

nature research

Corresponding author(s): Shaoqin Gong and Krishanu Saha

Last updated by author(s): Jul 20, 2019

Reporting Summary

Nature Research wishes to improve the reproducibility of the work that we publish. This form provides structure for consistency and transparency in reporting. For further information on Nature Research policies, see Authors & Referees and the Editorial Policy Checklist.

Statistics

For all statistical analyses, confirm that the following items are present in the figure legend, table legend, main text, or Methods section.

n/a	Confirmed
☐	☒ The exact sample size (*n*) for each experimental group/condition, given as a discrete number and unit of measurement
☐	☒ A statement on whether measurements were taken from distinct samples or whether the same sample was measured repeatedly
☐	☒ The statistical test(s) used AND whether they are one- or two-sided *Only common tests should be described solely by name; describe more complex techniques in the Methods section.*
☐	☒ A description of all covariates tested
☐	☒ A description of any assumptions or corrections, such as tests of normality and adjustment for multiple comparisons
☐	☒ A full description of the statistical parameters including central tendency (e.g. means) or other basic estimates (e.g. regression coefficient) AND variation (e.g. standard deviation) or associated estimates of uncertainty (e.g. confidence intervals)
☐	☒ For null hypothesis testing, the test statistic (e.g. *F*, *t*, *r*) with confidence intervals, effect sizes, degrees of freedom and *P* value noted *Give P values as exact values whenever suitable.*
☒	☐ For Bayesian analysis, information on the choice of priors and Markov chain Monte Carlo settings
☒	☐ For hierarchical and complex designs, identification of the appropriate level for tests and full reporting of outcomes
☒	☐ Estimates of effect sizes (e.g. Cohen's *d*, Pearson's *r*), indicating how they were calculated

Our web collection on statistics for biologists contains articles on many of the points above.

Software and code

Policy information about availability of computer code

Data collection	BD FACSDiva (version 8.0.2) was used to collect and FlowJo (v10) was used to analyze flow cytometry data. Deep sequencing data was analyzed using the CRISPR-RGEN Cas-Analyzer software. ImageJ (version 1.51s, NIH image) was used for image analysis. Adobe Illustrator (CC-2018) was used to composite images showing the whole mount RPE and muscle tissue. DLS Software (Zetasizer, version 7.01) was used for size and zeta potential measurement. Images were collected using NIS elements (Nikon).
Data analysis	All statistical analyses were performed on Graphpad Prism (version 7). ImageJ (version 1.51s, NIH image) was used for image analysis.

For manuscripts utilizing custom algorithms or software that are central to the research but not yet described in published literature, software must be made available to editors/reviewers. We strongly encourage code deposition in a community repository (e.g. GitHub). See the Nature Research guidelines for submitting code & software for further information.

Data

Policy information about availability of data

All manuscripts must include a data availability statement. This statement should provide the following information, where applicable:

- Accession codes, unique identifiers, or web links for publicly available datasets
- A list of figures that have associated raw data
- A description of any restrictions on data availability

The data that support the plots within this paper and other findings of this study are available from the corresponding authors upon reasonable request.

Field-specific reporting

Please select the one below that is the best fit for your research. If you are not sure, read the appropriate sections before making your selection.

☒ Life sciences ☐ Behavioural & social sciences ☐ Ecological, evolutionary & environmental sciences

For a reference copy of the document with all sections, see nature.com/documents/nr-reporting-summary-flat.pdf

Life sciences study design

All studies must disclose on these points even when the disclosure is negative.

Sample size	For retinal pigment epithelium studies, PBS (n=3), RNP (n=4), NC (n=6), or NC-ATRA (n=6). For muscle studies, n=4 for all conditions except PBS (n=2). Other experiments were done in biological triplicate. In previous studies we determined this sample size to be sufficient to ensure reproducibility.
Data exclusions	None
Replication	All the experimental findings were replicated with the number of replicates, animals and variation shown by n, SD, and/or SEM.
Randomization	The Ai14 mice of the same genotypes were randomly chosen to be in experimental or control groups according to experimental design.
Blinding	Generic labels without any chemical structures were used for all in vivo experiments. All data from in vivo experiments were collected and analyzed by at least two researchers using such a labeling strategy.

Behavioural & social sciences study design

All studies must disclose on these points even when the disclosure is negative.

Study description	*Briefly describe the study type including whether data are quantitative, qualitative, or mixed-methods (e.g. qualitative cross-sectional, quantitative experimental, mixed-methods case study).*
Research sample	*State the research sample (e.g. Harvard university undergraduates, villagers in rural India) and provide relevant demographic information (e.g. age, sex) and indicate whether the sample is representative. Provide a rationale for the study sample chosen. For studies involving existing datasets, please describe the dataset and source.*
Sampling strategy	*Describe the sampling procedure (e.g. random, snowball, stratified, convenience). Describe the statistical methods that were used to predetermine sample size OR if no sample-size calculation was performed, describe how sample sizes were chosen and provide a rationale for why these sample sizes are sufficient. For qualitative data, please indicate whether data saturation was considered, and what criteria were used to decide that no further sampling was needed.*
Data collection	*Provide details about the data collection procedure, including the instruments or devices used to record the data (e.g. pen and paper, computer, eye tracker, video or audio equipment) whether anyone was present besides the participant(s) and the researcher, and whether the researcher was blind to experimental condition and/or the study hypothesis during data collection.*
Timing	*Indicate the start and stop dates of data collection. If there is a gap between collection periods, state the dates for each sample cohort.*
Data exclusions	*If no data were excluded from the analyses, state so OR if data were excluded, provide the exact number of exclusions and the rationale behind them, indicating whether exclusion criteria were pre-established.*
Non-participation	*State how many participants dropped out/declined participation and the reason(s) given OR provide response rate OR state that no participants dropped out/declined participation.*
Randomization	*If participants were not allocated into experimental groups, state so OR describe how participants were allocated to groups, and if allocation was not random, describe how covariates were controlled.*

Ecological, evolutionary & environmental sciences study design

All studies must disclose on these points even when the disclosure is negative.

Study description	*Briefly describe the study. For quantitative data include treatment factors and interactions, design structure (e.g. factorial, nested, hierarchical), nature and number of experimental units and replicates.*
Research sample	*Describe the research sample (e.g. a group of tagged Passer domesticus, all Stenocereus thurberi within Organ Pipe Cactus National Monument), and provide a rationale for the sample choice. When relevant, describe the organism taxa, source, sex, age range and*

any manipulations. State what population the sample is meant to represent when applicable. For studies involving existing datasets, describe the data and its source.

Sampling strategy	Note the sampling procedure. Describe the statistical methods that were used to predetermine sample size OR if no sample-size calculation was performed, describe how sample sizes were chosen and provide a rationale for why these sample sizes are sufficient.
Data collection	Describe the data collection procedure, including who recorded the data and how.
Timing and spatial scale	Indicate the start and stop dates of data collection, noting the frequency and periodicity of sampling and providing a rationale for these choices. If there is a gap between collection periods, state the dates for each sample cohort. Specify the spatial scale from which the data are taken
Data exclusions	If no data were excluded from the analyses, state so OR if data were excluded, describe the exclusions and the rationale behind them, indicating whether exclusion criteria were pre-established.
Reproducibility	Describe the measures taken to verify the reproducibility of experimental findings. For each experiment, note whether any attempts to repeat the experiment failed OR state that all attempts to repeat the experiment were successful.
Randomization	Describe how samples/organisms/participants were allocated into groups. If allocation was not random, describe how covariates were controlled. If this is not relevant to your study, explain why.
Blinding	Describe the extent of blinding used during data acquisition and analysis. If blinding was not possible, describe why OR explain why blinding was not relevant to your study.

Did the study involve field work? ☐ Yes ☐ No

Field work, collection and transport

Field conditions	Describe the study conditions for field work, providing relevant parameters (e.g. temperature, rainfall).
Location	State the location of the sampling or experiment, providing relevant parameters (e.g. latitude and longitude, elevation, water depth).
Access and import/export	Describe the efforts you have made to access habitats and to collect and import/export your samples in a responsible manner and in compliance with local, national and international laws, noting any permits that were obtained (give the name of the issuing authority, the date of issue, and any identifying information).
Disturbance	Describe any disturbance caused by the study and how it was minimized.

Reporting for specific materials, systems and methods

We require information from authors about some types of materials, experimental systems and methods used in many studies. Here, indicate whether each material, system or method listed is relevant to your study. If you are not sure if a list item applies to your research, read the appropriate section before selecting a response.

Materials & experimental systems

n/a	Involved in the study
☐	☒ Antibodies
☐	☒ Eukaryotic cell lines
☒	☐ Palaeontology
☐	☒ Animals and other organisms
☒	☐ Human research participants
☒	☐ Clinical data

Methods

n/a	Involved in the study
☒	☐ ChIP-seq
☐	☒ Flow cytometry
☒	☐ MRI-based neuroimaging

Antibodies

Antibodies used	Primary antibodies: 1) Anti-Pax7 antibody: Supplier name: Developmental Studies Hybridoma Bank Catalog number: PAX7-c Clone name: N/A Lot number: N/A Dilution Used:1:30 2) Anti-RFP antibody Supplier name: Rockland Immunochemical Inc. Catalog number: 600-401-379 Clone name: N/A Lot number: 39707

Dilution Used: 1:300

Secondary antibody:
Donkey anti-rabbit IgG (H+L) conjugated with Alexa Fluor 546
Supplier name: Invitrogen
Catalog number: A10040
Clone name: N/A
Lot number: 2020130
Dilution used:1:250

Goat anti-mouse IgG1 conjugated with Alexa Fluor 488
Supplier name:Invitrogen,
Catalogue number: #A21121
Clone name: N/A
Dilution used: 1:250

Validation

All antibodies used have been tested and validated by the supplier and also by other researchers in the field. The dilution of each antibody was used based on a thorough prior investigation both in our labs and in other labs.

Pax7 antibody: For the validity in immunohistochemistry: Ohno et al. Nutrients 11:E869 (2019 Apr).
The supplier website (also provides the list of references to validate the antibody by other methods):
http://dshb.biology.uiowa.edu/PAX7

RFP antibody:
For the validity in immunohistochemistry: Probst et al. Genesis 55:e23043 (2017 Aug).
The supplier website (also provides the list of references to validate the antibody by other methods):
https://rockland-inc.com/store/Antibodies-to-GFP-and-Antibodies-to-RFP-600-401-379-O4L_24299.aspx?gclid=Cj0KCQjw1MXpBRDjARIsAHtdN-35xgnelbqXwBbZoWWyFEN1RnylGuCA99KB-W_h3F92KtHCLKuxEUwaAo7sEALw_wcB

Goat anti-mouse IgG1 conjugated with Alexa Fluor 488:
For the validity in immunohistochemistry: Fry et al., J Orthop Res 35(9):1876-1885 (2017 Jan).
The supplier website (also provides the list of references to validate the antibody by other methods):
https://www.thermofisher.com/antibody/product/Goat-anti-Mouse-IgG1-Cross-Adsorbed-Secondary-Antibody-Polyclonal/A-21121

Donkey anti-rabbit IgG (H+L) conjugated with Alexa Fluor 546:
For the validity in immunohistochemistry: Oh et al., Brain Struct Funct 222(5):2359-2378 (2017 Jul).
The supplier website (also provides the list of references to validate the antibody by other methods):
https://www.thermofisher.com/antibody/product/Donkey-anti-Rabbit-IgG-H-L-Highly-Cross-Adsorbed-Secondary-Antibody-Polyclonal/A10040

Eukaryotic cell lines

Policy information about cell lines

Cell line source(s)	Human embryonic kidney cells (HEK293): ATCC WA09 human embryonic stem cells (hESC): WiCell
Authentication	ATCC uses morphology, karyotyping, and PCR based approaches to confirm the identity of human cell lines and to rule out both intra- and interspecies contamination. Wicell uses Karyotyping and STR to authenticate cell line identity.
Mycoplasma contamination	All cell lines were tested negative for mycoplasma contamination every month of culture.
Commonly misidentified lines (See ICLAC register)	ICLAC-00063; HEK cells are commonly used in the CRISPR field to evaluate editing efficiency in vitro within human cells.

Palaeontology

Specimen provenance	*Provide provenance information for specimens and describe permits that were obtained for the work (including the name of the issuing authority, the date of issue, and any identifying information).*
Specimen deposition	*Indicate where the specimens have been deposited to permit free access by other researchers.*
Dating methods	*If new dates are provided, describe how they were obtained (e.g. collection, storage, sample pretreatment and measurement), where they were obtained (i.e. lab name), the calibration program and the protocol for quality assurance OR state that no new dates are provided.*

☐ Tick this box to confirm that the raw and calibrated dates are available in the paper or in Supplementary Information.

Animals and other organisms

Policy information about studies involving animals; ARRIVE guidelines recommended for reporting animal research

Laboratory animals	Ai14 mice (obtained from Jackson Labs) were used for these studies. Male mice of approximately 9 weeks of age were used for subretinal and intramuscular injections.
Wild animals	The study did not involve wild animals.
Field-collected samples	The study did not involve samples collected from field.
Ethics oversight	All mouse studies were carried out following protocols approved by the Institutional Animal Care and Use Committee at University of Wisconsin-Madison.

Note that full information on the approval of the study protocol must also be provided in the manuscript.

Human research participants

Policy information about studies involving human research participants

Population characteristics	*Describe the covariate-relevant population characteristics of the human research participants (e.g. age, gender, genotypic information, past and current diagnosis and treatment categories). If you filled out the behavioural & social sciences study design questions and have nothing to add here, write "See above."*
Recruitment	*Describe how participants were recruited. Outline any potential self-selection bias or other biases that may be present and how these are likely to impact results.*
Ethics oversight	*Identify the organization(s) that approved the study protocol.*

Note that full information on the approval of the study protocol must also be provided in the manuscript.

Clinical data

Policy information about clinical studies

All manuscripts should comply with the ICMJE guidelines for publication of clinical research and a completed CONSORT checklist must be included with all submissions.

Clinical trial registration	*Provide the trial registration number from ClinicalTrials.gov or an equivalent agency.*
Study protocol	*Note where the full trial protocol can be accessed OR if not available, explain why.*
Data collection	*Describe the settings and locales of data collection, noting the time periods of recruitment and data collection.*
Outcomes	*Describe how you pre-defined primary and secondary outcome measures and how you assessed these measures.*

ChIP-seq

Data deposition

☐ Confirm that both raw and final processed data have been deposited in a public database such as GEO.

☐ Confirm that you have deposited or provided access to graph files (e.g. BED files) for the called peaks.

Data access links *May remain private before publication.*	*For "Initial submission" or "Revised version" documents, provide reviewer access links. For your "Final submission" document, provide a link to the deposited data.*
Files in database submission	*Provide a list of all files available in the database submission.*
Genome browser session (e.g. UCSC)	*Provide a link to an anonymized genome browser session for "Initial submission" and "Revised version" documents only, to enable peer review. Write "no longer applicable" for "Final submission" documents.*

Methodology

Replicates	*Describe the experimental replicates, specifying number, type and replicate agreement.*
Sequencing depth	*Describe the sequencing depth for each experiment, providing the total number of reads, uniquely mapped reads, length of reads and whether they were paired- or single-end.*
Antibodies	*Describe the antibodies used for the ChIP-seq experiments; as applicable, provide supplier name, catalog number, clone name, and lot number.*

Peak calling parameters	*Specify the command line program and parameters used for read mapping and peak calling, including the ChIP, control and index files used.*
Data quality	*Describe the methods used to ensure data quality in full detail, including how many peaks are at FDR 5% and above 5-fold enrichment.*
Software	*Describe the software used to collect and analyze the ChIP-seq data. For custom code that has been deposited into a community repository, provide accession details.*

Flow Cytometry

Plots

Confirm that:

☒ The axis labels state the marker and fluorochrome used (e.g. CD4-FITC).

☒ The axis scales are clearly visible. Include numbers along axes only for bottom left plot of group (a 'group' is an analysis of identical markers).

☐ All plots are contour plots with outliers or pseudocolor plots.

☒ A numerical value for number of cells or percentage (with statistics) is provided.

Methodology

Sample preparation	Single cell suspensions from cultured cells were used for flow cytometry tests.
Instrument	BD FACSCanto II Flow Cytometor.
Software	BD FACSDiva was used for collection.
Cell population abundance	No mixed cell populations were used.
Gating strategy	Generally, cells was first gated on FSC/SSC. Singlet cells were usually gated using FSC-H and FSC-A.

☐ Tick this box to confirm that a figure exemplifying the gating strategy is provided in the Supplementary Information.

Magnetic resonance imaging

Experimental design

Design type	*Indicate task or resting state; event-related or block design.*
Design specifications	*Specify the number of blocks, trials or experimental units per session and/or subject, and specify the length of each trial or block (if trials are blocked) and interval between trials.*
Behavioral performance measures	*State number and/or type of variables recorded (e.g. correct button press, response time) and what statistics were used to establish that the subjects were performing the task as expected (e.g. mean, range, and/or standard deviation across subjects).*

Acquisition

Imaging type(s)	*Specify: functional, structural, diffusion, perfusion.*
Field strength	*Specify in Tesla*
Sequence & imaging parameters	*Specify the pulse sequence type (gradient echo, spin echo, etc.), imaging type (EPI, spiral, etc.), field of view, matrix size, slice thickness, orientation and TE/TR/flip angle.*
Area of acquisition	*State whether a whole brain scan was used OR define the area of acquisition, describing how the region was determined.*

Diffusion MRI ☐ Used ☐ Not used

Preprocessing

Preprocessing software	*Provide detail on software version and revision number and on specific parameters (model/functions, brain extraction, segmentation, smoothing kernel size, etc.).*
Normalization	*If data were normalized/standardized, describe the approach(es): specify linear or non-linear and define image types used for transformation OR indicate that data were not normalized and explain rationale for lack of normalization.*

Normalization template

Describe the template used for normalization/transformation, specifying subject space or group standardized space (e.g. original Talairach, MNI305, ICBM152) OR indicate that the data were not normalized.

Noise and artifact removal

Describe your procedure(s) for artifact and structured noise removal, specifying motion parameters, tissue signals and physiological signals (heart rate, respiration).

Volume censoring

Define your software and/or method and criteria for volume censoring, and state the extent of such censoring.

Statistical modeling & inference

Model type and settings

Specify type (mass univariate, multivariate, RSA, predictive, etc.) and describe essential details of the model at the first and second levels (e.g. fixed, random or mixed effects; drift or auto-correlation).

Effect(s) tested

Define precise effect in terms of the task or stimulus conditions instead of psychological concepts and indicate whether ANOVA or factorial designs were used.

Specify type of analysis: ☐ Whole brain ☐ ROI-based ☐ Both

Statistic type for inference
(See Eklund et al. 2016)

Specify voxel-wise or cluster-wise and report all relevant parameters for cluster-wise methods.

Correction

Describe the type of correction and how it is obtained for multiple comparisons (e.g. FWE, FDR, permutation or Monte Carlo).

Models & analysis

n/a	Involved in the study
☐	☐ Functional and/or effective connectivity
☐	☐ Graph analysis
☐	☐ Multivariate modeling or predictive analysis

Functional and/or effective connectivity

Report the measures of dependence used and the model details (e.g. Pearson correlation, partial correlation, mutual information).

Graph analysis

Report the dependent variable and connectivity measure, specifying weighted graph or binarized graph, subject- or group-level, and the global and/or node summaries used (e.g. clustering coefficient, efficiency, etc.).

Multivariate modeling and predictive analysis

Specify independent variables, features extraction and dimension reduction, model, training and evaluation metrics.